

Photoinduced energy- and electron-transfer processes in dinuclear ruthenium(II) and/or osmium(II) complexes connected by a linear rigid bis-chelating bridge

Luisa De Cola [#], Vincenzo Balzani [#], Francesco Barigelletti [§], Lucia Flamigni [§], Peter Belser [†], Stefan Bernhard [†]

[#] Dipartimento di Chimica "G. Ciamician" Università di Bologna, 40126 Bologna, Italy

[§] Istituto FRAE-CNR, via P. Gobetti 101, 40129 Bologna, Italy,

[†] Institut für Anorganische Chemie, Universität Freiburg, Freiburg, Switzerland

(Received March 3, 1995)

Abstract. A rigid and linear bridging ligand containing two 4,5-diazafluorene chelating units separated by an adamantane spacer (diazf-a-diazf) has been synthesized and its dinuclear complexes $[(bpy)_2Ru(diazf-a-diazf)Ru(bpy)_2]^{4+}$ ($Ru^{II} \cdot FAF \cdot Ru^{II}$), $[(bpy)_2Os(diazf-a-diazf)Os(bpy)_2]^{4+}$ ($Os^{II} \cdot FAF \cdot Os^{II}$), and $[(bpy)_2Ru(diazf-a-diazf)Os(bpy)_2]^{4+}$ ($Ru^{II} \cdot FAF \cdot Os^{II}$) have been prepared as PF_6^- salts. In these novel compounds, each Ru-based and Os-based unit displays its own absorption spectrum and electrochemical properties, regardless of the presence of a second metal-based unit. The luminescence properties have also been investigated and it has been shown that electronic energy transfer takes place in the mixed-metal $Ru^{II} \cdot FAF \cdot Os^{II}$ species at 77K from the Ru-based to the Os-based unit with rate constant $2.6 \cdot 10^8 \text{ s}^{-1}$. At room temperature the intrinsic decay of the Ru-based unit is too fast ($3.3 \cdot 10^9 \text{ s}^{-1}$) to allow the occurrence of energy transfer. Partial oxidation of the binuclear compounds $Ru^{II} \cdot FAF \cdot Os^{II}$ and $Os^{II} \cdot FAF \cdot Os^{II}$ by Ce^{IV} in acetonitrile–water solutions leads to the mixed-valence $Ru^{II} \cdot FAF \cdot Os^{III}$ and $Os^{II} \cdot FAF \cdot Os^{III}$ species where the oxidized metal-based unit quenches, by electron transfer, the luminescent excited state of the unit that is not oxidized. At room temperature, the rate constants for the excited state $*Ru^{II} \cdot FAF \cdot Os^{III} \rightarrow Ru^{III} \cdot FAF \cdot Os^{II}$ and $*Os^{II} \cdot FAF \cdot Os^{III} \rightarrow Os^{III} \cdot FAF \cdot Os^{II}$ processes are $8.3 \cdot 10^8 \text{ s}^{-1}$ and $3.9 \cdot 10^8 \text{ s}^{-1}$, respectively, and the rate constant for the back-electron-transfer process $Ru^{III} \cdot FAF \cdot Os^{II} \rightarrow Ru^{II} \cdot FAF \cdot Os^{III}$ is $2.9 \cdot 10^7 \text{ s}^{-1}$.

Introduction

Photoinduced energy- and electron-transfer processes in supramolecular species^{1–6} are currently the object of much interest since they can be exploited for the construction of sensors^{7,8} and light-harvesting^{1,5,6,9} and charge-separation^{1–3,5,6,10} devices. Progress in this field requires the availability of molecular components (building blocks) having well-defined structures and properties. As far as light- and/or redox-active units are concerned, much attention is presently focussed on $M(N-N)_3^{n+}$ complexes, where M is a metal ion of the second or third transition rows (in particular, Ru^{II} and Os^{II} and N-N is a bidentate bpy-type ligand (bpy = 2,2'-bipyridine)¹¹. When the active units are metal complexes, the connectors have to be bridging ligands. Several bridging ligands based on two bpy-type chelating units (directly coupled¹², or linked by flexible spacers like $-(CH_2)_n-$ chains¹³ or by rigid spacers like $-HC=CH-bco-HC=CH-$ ¹⁴ and $-C\equiv C-bco-C\equiv C-$ ¹⁵, (bco = bicyclo[2.2.2]octane) have been used. The choice of bridging ligands based on bpy chelating sites is very appropriate from an electronic viewpoint. In terms of structure, however, such a choice is not ideal because substitution of a single position in a bpy ligand cannot be symmetric with respect to the chelating site (Figure 1). As a consequence, with bridging ligands based on bpy units,

strict control of the structure of the dinuclear complex cannot be obtained even when rigid spacers are used (e.g., the metal–metal distance will depend on the reciprocal orientations of the two chelating sites).

Continuing our investigations in this field, we have designed a novel bis-chelating bridging ligand (diazf-a-diazf, Figure 1) based on two 4,5-diazafluorene^a units connected by an adamantane spacer. This bridging ligand is rigid and leads to dinuclear species in which the two metals and the spacer lie in a row. This structural arrangement is reminiscent of that obtained with tridentate tpy-type ligands (tpy = 2,2':6',2''-terpyridine) bearing a single substituent in the 4' position (Figure 1)¹⁶.

In this paper we report the synthesis of the new diazf-a-diazf bridging ligand and its dinuclear complexes $[(bpy)_2Ru(diazf-a-diazf)Ru(bpy)_2]^{4+}$ ($Ru^{II} \cdot FAF \cdot Ru^{II}$), $[(bpy)_2Os(diazf-a-diazf)Os(bpy)_2]^{4+}$ ($Os^{II} \cdot FAF \cdot Os^{II}$), and $[(bpy)_2Ru(diazf-a-diazf)Os(bpy)_2]^{4+}$ ($Ru^{II} \cdot FAF \cdot Os^{II}$). In all these complexes the metal–metal distance is 16 Å as evaluated by molecular modelling using ALCHEMY. The electrochemical properties, absorption spectra, and luminescence behavior (emission and excita-

^a IUPAC name: 5H-cyclopenta[2,1-b:3,4-b']dipyridine.

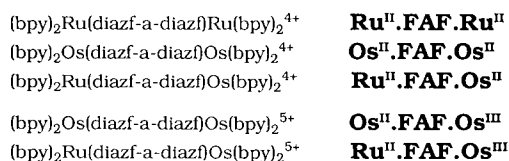
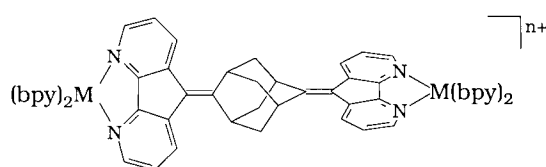
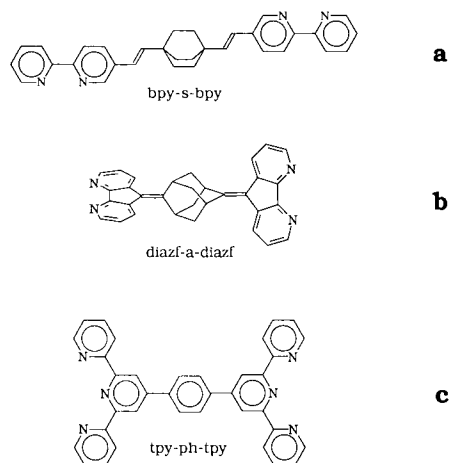


Figure 1. Top: schematic representation of a bis-bipyridine bridging ligand (a)¹⁴, of the novel diazf-a-diazf bridging ligand (b), and of a tpy-based bridging ligand (c)¹⁶; bottom: formulae of the complexes investigated in this paper and abbreviations used.

tion spectra, excited state lifetimes) and, for **Ru^{II}·FAF·Os^{II}**, intercomponent energy transfer are reported and discussed. By partial oxidation of the binuclear compounds **Ru^{II}·FAF·Os^{II}** and **Os^{II}·FAF·Os^{II}** we have also obtained the mixed-valence **Ru^{II}·FAF·Os^{III}** and **Os^{II}·FAF·Os^{III}** species, with which photoinduced electron-transfer processes have been investigated.

Experimental

Equipment and methods

¹H-NMR (300 MHz) and ¹³C-NMR (75.4 MHz) spectra were recorded with a Varian Gemini 300 instrument using the proton impurities of the deuterated solvents as reference. Chemical shifts are reported in ppm on the δ scale. Mass-spectral data were obtained with a VG Instruments 7070E mass spectrometer equipped with a FAB inlet system. The FAB measurements were carried out in a 3-nitrobenzyl alcohol matrix. Xenon atoms were used for the bombardment (8 kV). Electrochemical measurements were carried out at room temperature (~ 298 K) by using a PAR 273A Electrochemical Analysis System with the 270 Research Electrochemistry Software. Cyclic voltammograms were obtained in acetonitrile solutions using a micro cell equipped with a stationary platinum-disk electrode, a platinum-disk counter electrode, and SCE reference electrode with tetrabutylammonium hexafluorophosphate as supporting electrolyte. In all cases $[Ru(bpy)_3](PF_6)_2$ was used as a standard, taking its oxidation potential as +1260 mV vs SCE¹⁷. The electrochemical window examined was between +1.6 and -2.0 volts. Scanning speed was 200 mV/s. Half-wave potentials were calculated as an average of the cathodic and anodic peaks. All reagents and solvents were commercial samples obtained by Fluka-Chemie AG or Aldrich, and, unless otherwise stated, they were used as supplied. Absorption spectra were measured in acetonitrile solution at room

temperature with a Perkin-Elmer Lambda 6 spectrophotometer. Luminescence experiments were performed in air-equilibrated acetonitrile solution at room temperature and in freshly distilled butyronitrile at 77K. Uncorrected luminescence spectra were obtained with a Perkin-Elmer LS 50 spectrofluorimeter. When necessary for comparison purposes, the luminescence intensity values were corrected to take into account the different absorbance values of the two solutions. Luminescence-decay measurements on the nanosecond scale were performed with an Edinburgh and an IBH single-photon-counting equipment. Selection of excitation and emission wavelength was done by using monochromators and cut-off or band-pass optical filters. Analysis of the decay curves was performed by employing either home-made non-linear iterative programs or programs provided by the manufacturers.

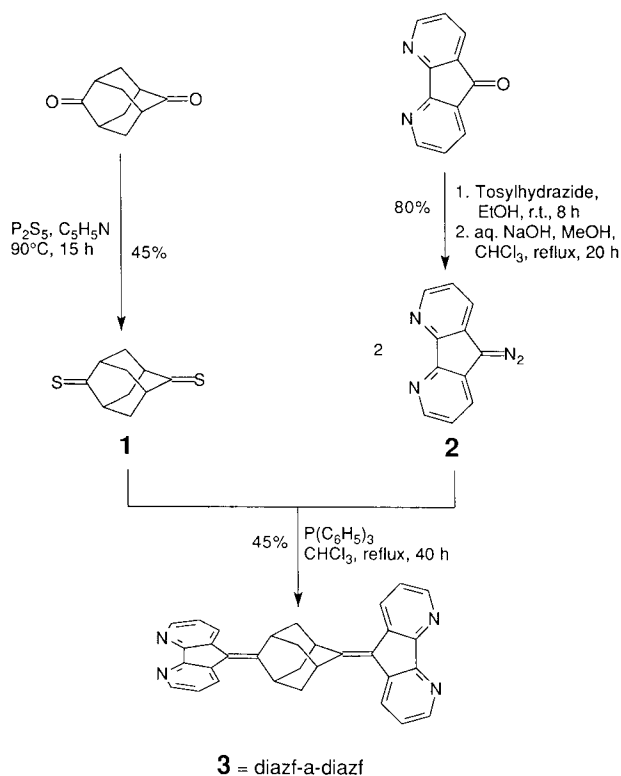
Flash-photolysis experiments were carried out with a Nd:YAG laser (J.K. Lasers) with 20 ns pulse duration. The third harmonic (λ 355 nm) with an energy of 8 mJ/pulse was used to excite the samples. The probe beam generated by a pulsed Xenon arc lamp crossed the irradiated area at right angles to the excitation. The light transmitted was focussed on the entrance slit of a monochromator and detected by an R936 Hamamatsu photomultiplier. Acquisition and processing of signals was obtained by a transient digitizer (Tektronix R7912) in conjunction with a PC.

Picosecond fluorescence lifetimes were detected with an apparatus based on a mode-locked, cavity-dumped Nd:YAG laser (Continuum PY62-10) and a streak camera (Hamamatsu C1587) equipped with a fast single-sweep unit (M1952). The third harmonic (λ 355 nm) with an energy of 4 mJ/pulse and a pulse duration of 35 ps was used to excite the samples. The light emitted was collected and fed into the entrance of a spectrograph (HR 250 Jobin-Yvon) and then focussed on the slit of the streak camera. Acquisition and processing of the streak images were performed via cooled CCD camera (Hamamatsu C3140) and related software running on a PC. Typical images were the average of 250–1000 events. Data of emission intensity vs time over 20 nm around the maximum were averaged. The analysis of such profiles was performed with standard iterative non-linear procedures. Time resolution of the system was 30 ps. Calibration of the wavelength was achieved by using the Nd:YAG laser emission harmonics.

Estimated errors are as follows: band maxima, ± 2 nm; relative luminescence intensity $\pm 20\%$; lifetimes, $\pm 10\%$.

Preparation of the bridging ligand

The route followed to prepare the bridging ligand is shown in Scheme 1.



Scheme 1.

Adamantane-2,6-dione was synthesized according to Janku and Landa et al.¹⁸. The second precursor 4,5-diazafluoren-9-one was synthesized according to the method of Cherry et al.¹⁹. The synthesis of adamantane-2,6-dithione was performed according to the method of Greidanus²⁰.

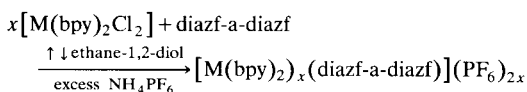
Adamantane-2,6-dithione (1) To a 25 ml two-necked round-bottom flask equipped with a magnetic stirring bar were added adamantane-2,6-dione (0.525 g, 3.20 mmol) and anhydrous pyridine (10 ml, H₂O < 0.05%). Under argon atmosphere P₂S₅ (0.356 g, 1.6 mmol) was added portion-wise (30 min) at 90°C. The reaction mixture was stirred vigorously for 15 h at this temperature; the initially yellow solution changed to orange during this process. After cooling to room temperature the solution was added to hexane (100 ml) and the mixture was extracted with water (3 × 100 ml), 2N HCl (3 × 100 ml) and again twice with water (100 ml). After drying (MgSO₄) the solvent was removed in vacuum to give 0.535 g of crude **1**. The orange solid was purified by sublimation (1 mbar, 120°C) to give pure **1** as orange crystals. Yield 0.282 g (**1**, 1.44 mmol, 45%). MS (EI, 70 eV): *m/z* 196 (M⁺), 163 (M⁺ - SH), 129 (M⁺ - 2 SH). ¹H-NMR (CDCl₃): δ, *J* (Hz) 2.32–2.38 (m, 8H), 3.48–3.55 (m, 4H). ¹³C-NMR (CDCl₃): δ 43.1 (CH₂), 55.4 (CH), 263.8 (C = S).

9-Diazo-4,5-diazafluorene (2) Tosylhydrazide (2.00 g, 10.73 mmol) and 4,5-diazafluoren-9-one (1.00 g, 5.49 mmol) were dissolved in anhydrous EtOH (100 ml) and stirred for 8 h at room temperature. The resulting yellow suspension was filtered and washed with a small amount of EtOH. The solid was dissolved in 200 ml CHCl₃, 200 ml MeOH and 100 ml NaOH (2 M). The mixture was then heated to reflux for 20 h. After cooling the organic layer was separated, washed with water (100 ml), dried (MgSO₄), treated with charcoal and filtered. The reddish brown solution was concentrated by distillation to give a brown solid. Yield 0.85 g (**2**, 4.38 mmol, 80%). The compound is not stable and should be used within a few days of production. MS (EI, 70 eV): *m/z* 194 (M⁺), 166 (M⁺ - N₂). ¹H-NMR (CDCl₃): δ, *J* (Hz) 7.36 (dd, 2H, ³*J* 8.0, ³*J* 4.7), 7.88 (dd, 2H, ³*J* 8.0, ⁴*J* 1.4), 8.68 (dd, 2H, ³*J* 4.7, ⁴*J* 1.4).

9,9'-(Adamantane-2,6-diyliidene)bis[4,5-diazafluorene] (3) To a 5-ml two-necked pear-shaped flask equipped with a magnetic stirring bar was added **1** (98 mg, 0.50 mmol), **2** (194 mg, 1.00 mmol) and chloroform (4 ml). The brown solution was heated to reflux for 15 h under an argon atmosphere. After 2 h, a brown precipitation was formed. To the cooled brown suspension, triphenylphosphine (350 mg, 1.33 mmol) was added. The reaction mixture was refluxed under argon atmosphere for another 24 h. After cooling the suspension was filtered, washed with a small amount of CHCl₃ and the white solid dried in vacuum. Yield 103 mg (**3**, 0.22 mmol, 45%). MS (FAB): *m/z* 465 (M⁺ + 1). ¹H-NMR (CDCl₃): δ, *J* (Hz) 2.47 (s, 8H), 4.16 (s, 4H), 7.30 (dd, 2H, ³*J* 8.0, ³*J* 4.8), 8.22 (dd, 2H, ³*J* 8.0, ⁴*J* 1.3), 8.68 (dd, 2H, ³*J* 4.8, ⁴*J* 1.3). ¹³C-NMR (CDCl₃): δ 35.2, 41.1, 122.4, 122.6, 131.6, 133.2, 149.0, 156.9, 159.8.

Preparation of the metal complexes

The homo-metallic complexes of the bridging ligand **3**, hereafter called diazf-a-diazf, were prepared according to the general one-step reaction:



$$x = 1, 2 \quad \text{M} = \text{Ru}, \text{Os}$$

The mixed-metal [(bpy)₂Ru(diazf-a-diazf)Os(bpy)₂](PF₆)₄ compound was prepared in a two-step reaction. The monomeric [(bpy)₂Os(diazf-a-diazf)](PF₆) species, synthesized in the first step, with butane-1,4-diol as solvent, was reacted with a stoichiometric amount of Ru(bpy)₂Cl₂ as indicated above.

Commercially available 2,2'-bipyridine and RuCl₃·3H₂O were used as received. The precursors Ru(bpy)₂Cl₂·2H₂O²¹ and Os(bpy)₂Cl₂²² were prepared according to literature procedures. The solvents and reactants were of the highest purity commercially available and were used as received.

[(bpy)₂Ru(diazf-a-diazf)Ru(bpy)₂](PF₆)₄ (Ru^{II}·FAF·Ru^{II}). A mixture of 0.030 g (0.0646 mmol) diazf-a-diazf (**3**) and 0.067 g Ru(bpy)₂Cl₂·2H₂O in 3 ml ethane-1,2-diol/water (5%) was refluxed in a microwave oven for 8 min²³. Water (30 ml) was added to the cold reaction mixture and the solution was filtered. A solution of 1.0 g NH₄PF₆ dissolved in 5 ml water was added and the precipitate filtered off and dried at 80°C. The complex was purified on a

preparative silica-gel plate²⁴ (PTCL) (silica gel) with a 3/2 mixture of EtOH/water/NaCl (1/1/0.1) and DMF/water/NH₄Cl (4/1/0.1) as eluting solvent, to form an orange solid (0.095 g, 79%). MS (FAB): *m/z* 1728 (M⁺ - PF₆⁻), *m/z* 1582 (M⁺ - 2 PF₆⁻). ¹H-NMR (CD₃CN): δ, *J* (Hz) 2.61 (s, 8 H, CH₂-adamantane), 4.32 (s, 4 H, CH-adamantane), the following protons are attributed to bpy-H and diazf-a-diazf-H, 7.56–7.61 (m, 12 H), 7.80 (d, 4 H, ³*J* 5.4), 8.18–8.28 (m, 12 H), 8.29 (d, 4 H, ³*J* 5.0), 8.76 (d, 4 H, ³*J* 7.25), 8.81 (d, 8 H, ³*J* 8.24).

[(bpy)₂Os(diazf-a-diazf)Os(bpy)₂](PF₆)₄ (Os^{II}·FAF·Os^{II}) A solution of 0.030 g (0.0646 mmol) diazf-a-diazf (**3**) and 0.074 g (0.129 mmol) Os(bpy)₂Cl₂ in 3 ml ethane-1,2-diol/water (5%) was refluxed for 8 min in a microwave oven. After adding 30 ml water to the cold reaction mixture, the compound was isolated and purified as described before. The compound produced was an olive-green solid (0.098 g, 74%). MS (FAB): *m/z* 1905 (M⁺ - PF₆⁻), *m/z* 1759 (M⁺ - 2 PF₆⁻). ¹H-NMR (CD₃CN): δ, *J* (Hz) 2.61 (s, 8 H, CH₂-adamantane), 4.32 (s, 4 H, CH-adamantane), the following protons are attributed to bpy-H and diazf-a-diazf-H, 7.46–7.56 (m, 12 H), 7.75 (d, 4 H, ³*J* 5.2), 7.97 (dd, 8 H, ³*J* 7.8), 8.12 (d, 4 H, ³*J* 5.8), 8.16 (d, 4 H, ³*J* 5.8), 8.52 (d, 4 H, ³*J* 8.2), 8.78 (d, 8 H, ³*J* 8.2).

[(bpy)₂Ru(diazf-a-diazf)Os(bpy)₂](PF₆)₄ (Ru^{II}·FAF·Os^{II}) A mixture of 0.030 g (0.0646 mmol) diazf-a-diazf (**3**) and 20 ml butane-1,4-diol was heated in microwave oven for 2 min. Os(bpy)₂Cl₂ (0.037 g, 0.0646 mmol) was added in three portions to the clear solution. After each addition, the reaction mixture was heated in the microwave oven for 2 min. After the last addition, the solution was again treated for 4 min in the microwave oven. The solvent was evaporated, the metal complex dissolved in water, filtered and the solution extracted twice with dichloromethane. A solution of 1.0 g NH₄PF₆ dissolved in 5 ml water was added to the aqueous part, the precipitate filtered off and dried in a furnace at 80°C. The complex was purified on a preparative thin-layer plate and isolated as described above. The isolated yield of the olive-green [Os(bpy)₂(diazf-a-diazf)](PF₆)₂ complex was 0.043 g (53%). The [Os(bpy)₂(diazf-a-diazf)](PF₆)₂ complex was dissolved in a mixture of 0.018 g (0.0342 mmol) of Ru(bpy)₂Cl₂·2H₂O and 3 ml ethane-1,2-diol/water (5%) and heated for 8 min in a microwave oven. Water (30 ml) was added to the cold reaction mixture and the solution was filtered. A solution of 1.0 g NH₄PF₆ dissolved in 5 ml water was added, the precipitate filtered off and dried at 80°C. The complex was purified as described for the compound Ru^{II}·FAF·Ru^{II}, to give an olive-green solid (0.034 g, 50%). ¹H-NMR (CD₃CN): δ, *J* (Hz) 2.60 (s, 8 H, CH₂-adamantane), 4.32 (s, 4 H, CH-adamantane), the following protons are attributed to bpy-H and diazf-a-diazf-H, 7.46–7.60 (m, 12 H), 7.75 (d, 2 H, ³*J* 5.2), 7.79 (d, 2 H, ³*J* 5.0), 7.97 (dd, 4 H, ³*J* 7.6), 8.11–8.22 (m, 10 H), 8.28 (d, 2 H, ³*J* 5.0), 8.52 (d, 2 H, ³*J* 7.9), 8.70 (d, 2 H, ³*J* 7.7), 8.79 (dd, 8 H, ³*J* 8.2).

Results

Electrochemical behavior

The electrochemical potentials for the first oxidation and reduction processes of the compounds are collected in Table I, where the data for Ru(bpy)₃²⁺ and Os(bpy)₃²⁺ are also reported for purposes of comparison.

Absorption spectra

The absorption spectra of the three dinuclear complexes in acetonitrile solution at room temperature are shown in

Table I Electrochemical data ^a. Redox potentials, *V* ^b.

Complex	Oxidation		Reduction
	Ru	Os	
Ru ^{II} ·FAF·Ru ^{II}	+1.265 [2] (90)	–	–1.285 [2] (120)
Os ^{II} ·FAF·Os ^{II}	–	+0.800 [2] (85)	–1.245 [2] (75)
Ru ^{II} ·FAF·Os ^{II}	+1.260 [1] (80)	+0.800 [1] (80)	–1.275 [2] (115)
Ru(bpy) ₃ ²⁺ ^c	+1.260 [1] (95)	–	–1.35 [1] (90)
Os(bpy) ₃ ²⁺ ^d	–	+0.83 [1] (80)	–1.28 [1] (80)

^a Acetonitrile solution, room temperature; potential values vs. SCE.

^b Relative current intensity within square brackets []; peak separation within parenthesis ()

^c Ref. 11a. ^d Ref. 11b.

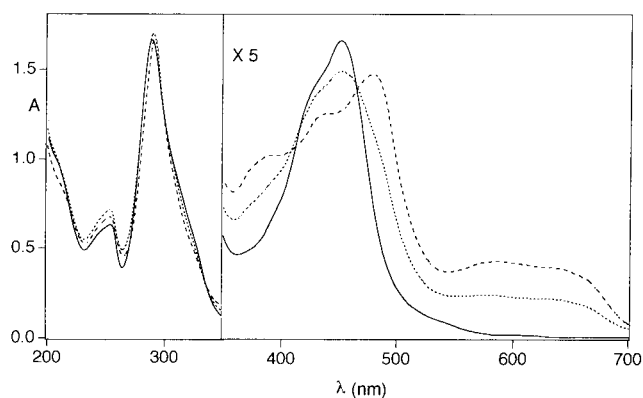


Figure 2. Absorption spectra in acetonitrile solution ($1.5 \cdot 10^{-5}$ M) at room temperature of $\text{Ru}^{\text{II}} \cdot \text{FAF} \cdot \text{Ru}^{\text{II}}$ (—), $\text{Ru}^{\text{II}} \cdot \text{FAF} \cdot \text{Os}^{\text{II}}$ (---), and $\text{Os}^{\text{II}} \cdot \text{FAF} \cdot \text{Os}^{\text{II}}$ (- - -).

Figure 2. The absorption spectrum of the mixed metal $\text{Ru}^{\text{II}} \cdot \text{FAF} \cdot \text{Os}^{\text{II}}$ compound is equal to the spectrum of the 1/1 mixture of its homodinuclear “parent” compounds $\text{Ru}^{\text{II}} \cdot \text{FAF} \cdot \text{Ru}^{\text{II}}$ and $\text{Os}^{\text{II}} \cdot \text{FAF} \cdot \text{Os}^{\text{II}}$.

Luminescence

The steady-state luminescence spectra of the three compounds in acetonitrile solution at room temperature and in butyronitrile solution at 77K are displayed in Figures 3 and 4, respectively. The inset of Figure 3 shows the time-resolved (gate: 0–430 ps) emission spectrum of $\text{Ru}^{\text{II}} \cdot \text{FAF} \cdot \text{Ru}^{\text{II}}$. A summary of the photophysical data is given in Table II, where the corresponding data for the $\text{Ru}(\text{bpy})_3^{2+}$ (Ref. 11a), $\text{Os}(\text{bpy})_3^{2+}$ (Ref. 11b), and $\text{Ru}(\text{bpy})_2(4,5\text{-diazafluorene})^{2+}$ (Refs. 19,25,26) model compounds are also shown. The luminescence decay was strictly monoexponential unless otherwise noted.

As shown in Figure 3, the luminescent behavior of $\text{Ru}^{\text{II}} \cdot \text{FAF} \cdot \text{Ru}^{\text{II}}$ at room temperature has been investigated with different techniques. In view of its very weak intensity, the luminescence band observed by steady-state techniques with λ_{max} ca. 610 nm could in fact be due to a small amount of a strongly luminescent impurity rather than to a weak emission of $\text{Ru}^{\text{II}} \cdot \text{FAF} \cdot \text{Ru}^{\text{II}}$. The problem of bona fide weak emissions in Ru^{II} -polypyridine complexes has always to be taken into consideration in view of the strong luminescence of several members of this family²⁷. A very weak luminescence band observed for the mononuclear model compound $\text{Ru}(\text{bpy})_2(4,5\text{-diazafluorene})^{2+}$ was initially thought to be a genuine emission¹⁹, but was later attributed to an impurity²⁵. It is well known^{11a} that in the family of Ru^{II} -polypyridine complexes the strongly luminescent species have lifetimes of

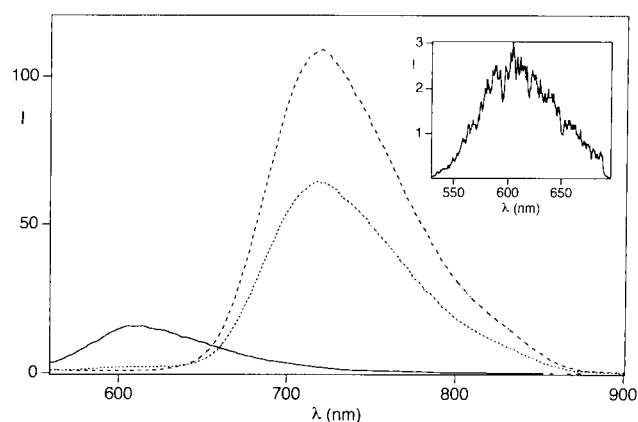


Figure 3. Luminescence spectrum in acetonitrile solution at room temperature of $\text{Ru}^{\text{II}} \cdot \text{FAF} \cdot \text{Ru}^{\text{II}}$ (—), $\text{Ru}^{\text{II}} \cdot \text{FAF} \cdot \text{Os}^{\text{II}}$ (---), and $\text{Os}^{\text{II}} \cdot \text{FAF} \cdot \text{Os}^{\text{II}}$ (- - -). The inset shows the time-resolved spectrum of $\text{Ru}^{\text{II}} \cdot \text{FAF} \cdot \text{Ru}^{\text{II}}$ (for details, see text).

the order of 10^2 – 10^3 ns, and that the weakly luminescent species have lifetimes of the order of 1 ns.

Therefore, lifetime measurements can help to elucidate the problem of luminescent impurities. We have found that the weak luminescence observed for $\text{Ru}^{\text{II}} \cdot \text{FAF} \cdot \text{Ru}^{\text{II}}$ shows a biexponential decay, corresponding to lifetimes of 170 ns and 300 ps. This suggests the presence of both a (long-lived) luminescent impurity and a genuine (short-lived) $\text{Ru}^{\text{II}} \cdot \text{FAF} \cdot \text{Ru}^{\text{II}}$ emission. The time-resolved spectra taken with a gate of 430 ps after the pulse show a maximum at 605 nm, which can be assigned to $\text{Ru}^{\text{II}} \cdot \text{FAF} \cdot \text{Ru}^{\text{II}}$. In fact, in this time scale, the emission of the long-lived impurity appears as a very low background which cannot influence the spectral shape.

In rigid matrix at 77K, $\text{Ru}^{\text{II}} \cdot \text{FAF} \cdot \text{Ru}^{\text{II}}$ shows a strong and long-lived emission, very similar to that exhibited by $\text{Ru}(\text{bpy})_3^{2+}$ or $\text{Ru}(\text{bpy})_2(4,5\text{-diazafluorene})^{2+}$. The luminescence of $\text{Os}^{\text{II}} \cdot \text{FAF} \cdot \text{Os}^{\text{II}}$ is also very similar to that exhibited by $\text{Os}(\text{bpy})_3^{2+}$. In the heteronuclear $\text{Ru}^{\text{II}} \cdot \text{FAF} \cdot \text{Os}^{\text{II}}$ compound both the Ru-based and Os-based luminescence bands are present, but the Ru-based emission has very low intensity and short lifetime.

Generation of mixed-valence compounds and their properties

Addition of a standardized Ce^{IV} solution (see experimental section) to a $5 \cdot 10^{-5}$ M solution of $\text{Os}^{\text{II}} \cdot \text{FAF} \cdot \text{Os}^{\text{II}}$ and $\text{Ru}^{\text{II}} \cdot \text{FAF} \cdot \text{Os}^{\text{II}}$ caused strong changes in the absorption spectra, fully comparable to those obtained for oxidation of $\text{Os}(\text{bpy})_3^{2+}$. $\text{Os}(\text{bpy})_3^{3+}$ shows an absorption band in the visible region with λ_{max} 563 nm, with small molar

Table II Luminescence data.

Complex	298K ^a					77K ^b			
	Ru		Os			Ru		Os	
	λ_{max} (nm)	τ (ns)	λ_{max} (nm)	τ (ns)	I_{rel}^c	λ (nm)	τ (μ s)	λ (nm)	τ (μ s)
$\text{Ru}^{\text{II}} \cdot \text{FAF} \cdot \text{Ru}^{\text{II}}$	605 ^d	0.300	—	—	—	577	5.5	—	—
$\text{Os}^{\text{II}} \cdot \text{FAF} \cdot \text{Os}^{\text{II}}$	—	—	720	41	100	—	—	710	1.1
$\text{Ru}^{\text{II}} \cdot \text{FAF} \cdot \text{Os}^{\text{II}}$	605 ^d	0.290	720	40	50	577	0.0039	703	1.1
$\text{Ru}(\text{bpy})_2(4,5\text{-diazafluorene})^{2+}$	— ^e	0.07 ^f	—	—	—	574	5.9	—	—
$\text{Ru}(\text{bpy})_3^{2+}$	615	170	—	—	—	582	5.0	—	—
$\text{Os}(\text{bpy})_3^{3+}$	—	—	743	49	—	—	—	710	0.83

^a Air-equilibrated acetonitrile solution. ^b Butyronitrile solution. ^c Excitation was performed at 464 nm, which is an isosbestic point between the Ru-based and Os-based units; for comparison purposes, the luminescence intensity of $\text{Os}^{\text{II}} \cdot \text{FAF} \cdot \text{Os}^{\text{II}}$ at 720 nm was taken as 100. ^d Determined by time-resolved spectra (see text). ^e Covered by an impurity emission (Ref. 19,26). ^f Evaluated from extrapolation of low-temperature data (Ref. 26).

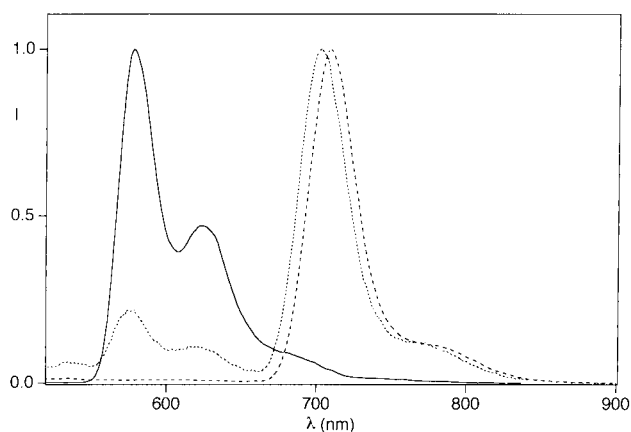


Figure 4. Normalized luminescence spectra in butyronitrile rigid glass at 77K of $\text{Ru}^{\text{II}} \cdot \text{FAF} \cdot \text{Ru}^{\text{II}}$ (—), $\text{Ru}^{\text{II}} \cdot \text{FAF} \cdot \text{Os}^{\text{II}}$ (---) and $\text{Os}^{\text{II}} \cdot \text{FAF} \cdot \text{Os}^{\text{II}}$ (- - -).

absorption coefficient ($585 \text{ M}^{-1} \text{ cm}^{-1}$)²⁸. This band is assigned to doublet \rightarrow doublet ligand-to-metal charge transfer (LMCT) transitions from a π orbital of the ligands to the t_{2g} (in octahedral symmetry) metal orbitals, which have an empty place because of the d^5 electronic configuration of Os^{III} .

For $\text{Os}^{\text{II}} \cdot \text{FAF} \cdot \text{Os}^{\text{II}}$, the absorbance in the 600-nm spectral region decreased linearly with increasing number of added oxidation equivalents and disappeared after addition of two equivalents of oxidant. For $\text{Ru}^{\text{II}} \cdot \text{FAF} \cdot \text{Os}^{\text{II}}$, the addition of one equivalent of oxidant again caused the disappearance of the Os-based absorption, as expected because of the different oxidation potentials of the Os-based and Ru-based moieties (Table I). For this species, if allowance is made for the changes due to the oxidation of the Os-based moiety, the Ru-based absorbance at 450 nm remains unchanged after addition of one equivalent of oxidant.

It is well known that Os^{III} -polypyridine complexes do not exhibit luminescence¹⁵. For $\text{Ru}^{\text{II}} \cdot \text{FAF} \cdot \text{Os}^{\text{II}}$, the addition of one equivalent of oxidant quenches completely the Os-based luminescence, whereas a weak Ru-based luminescence, with lifetime 240 ps, is still present. Flash-photolysis experiments showed that the quenching of the Ru-based luminescent excited state in $^* \text{Ru}^{\text{II}} \cdot \text{FAF} \cdot \text{Os}^{\text{III}}$ leads to a transient species which exhibits the absorption spectrum shown in Figure 5. Comparison with the spectra of Figure 2 clearly shows that this transient is the $\text{Ru}^{\text{III}} \cdot \text{FAF} \cdot \text{Os}^{\text{II}}$ species, which decays to $\text{Ru}^{\text{II}} \cdot \text{FAF} \cdot \text{Os}^{\text{III}}$ with rate constant $2.9 \cdot 10^7 \text{ s}^{-1}$ (Figure 5, inset).

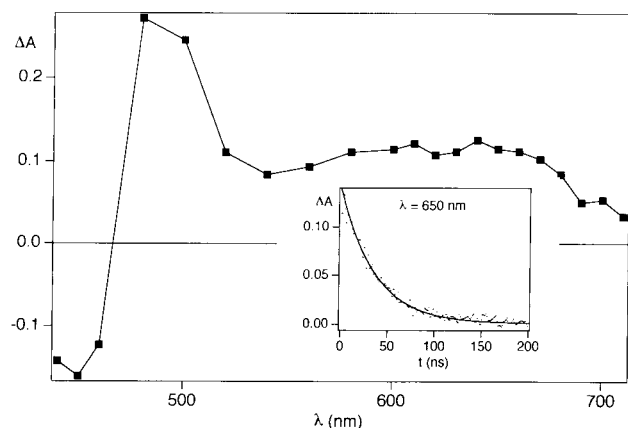


Figure 5. Transient absorption spectrum of the product obtained upon excitation of the Ru-based moiety of $\text{Ru}^{\text{II}} \cdot \text{FAF} \cdot \text{Os}^{\text{III}}$. The inset shows the absorbance decay at 650 nm.

For $\text{Os}^{\text{II}} \cdot \text{FAF} \cdot \text{Os}^{\text{II}}$, the decrease in the luminescence intensity upon addition of the oxidant was not linear because oxidation leads to a mixture of $\text{Os}^{\text{II}} \cdot \text{FAF} \cdot \text{Os}^{\text{II}}$, $\text{Os}^{\text{II}} \cdot \text{FAF} \cdot \text{Os}^{\text{III}}$, and $\text{Os}^{\text{III}} \cdot \text{FAF} \cdot \text{Os}^{\text{III}}$. Luminescence-lifetime measurements after addition of 1.2 equivalents of oxidant gave a biexponential decay with lifetimes of 41 ns and 2.4 ns, assigned to $^* \text{Os}^{\text{II}} \cdot \text{FAF} \cdot \text{Os}^{\text{II}}$ and $^* \text{Os}^{\text{II}} \cdot \text{FAF} \cdot \text{Os}^{\text{III}}$, respectively.

For the mixed-valence species, absorption measurements up to 1400 nm excluded the presence of intervalence transfer bands with $\epsilon > 50 \text{ M}^{-1} \cdot \text{cm}^{-1}$.

Discussion

Properties of the components and intercomponent interactions

In oligonuclear complexes electronic interactions between the mononuclear components may range from very strong (with profound changes in the spectroscopic and electrochemical properties on passing from mononuclear to oligonuclear species) to very weak (with almost equal properties for separated and bridged units), depending on the type of bridge. In any case, comparison with the behavior of model mononuclear compounds is very useful. Extensive investigations performed on mononuclear Ru^{II} and Os^{II} complexes¹¹ have shown that: (i) oxidation is metal-centered; (ii) Os^{II} is easier to oxidize than Ru^{II} ; (iii) reduction is ligand-centered; (iv) the absorption bands in the visible region are due to spin-allowed metal-to-ligand charge-transfer (MLCT) transitions (and related spin-forbidden transitions for Os^{II} complexes); (v) luminescence takes place from the lowest energy excited state which formally is a triplet MLCT level; (vi) the luminescent excited state is rapidly populated with unitary efficiency regardless of the excitation wavelength; (vii) at room temperature, the main radiation-less decay channel for the luminescent $^3\text{MLCT}$ level of the Ru^{II} complexes is a thermally activated crossing to an upper triplet ligand field (^3LF) level which undergoes fast decay to ground state and/or reaction products; for the Os^{II} complexes this deactivation channel is unimportant.

Cherry, Schmehl and co-workers^{19,25,26} have thoroughly investigated the spectroscopic and excited-state behavior of the $\text{Ru}(\text{bpy})_2(4,5\text{-diazafluorene})^{2+}$ complex, which is the Ru-based unit present in $\text{Ru}^{\text{II}} \cdot \text{FAF} \cdot \text{Ru}^{\text{II}}$, $\text{Ru}^{\text{II}} \cdot \text{FAF} \cdot \text{Os}^{\text{II}}$, and $\text{Ru}^{\text{II}} \cdot \text{FAF} \cdot \text{Os}^{\text{III}}$. They have demonstrated that, since the chelating bite of 4,5-diazafluorene is not as good as that of bpy for octahedral coordination, replacement of one bpy by $\text{Ru}(\text{bpy})_3^{2+}$ by the 4,5-diazafluorene ligand decreases strongly the energy of the ligand field excited states, whereas it does not substantially affect the MLCT levels. As a consequence the activation barrier between the luminescent $^3\text{MLCT}$ level and the upper ^3LF level decreases from ca. 3900 cm^{-1} for $\text{Ru}(\text{bpy})_3^{2+}$ to ca. 2000 cm^{-1} for $\text{Ru}(\text{bpy})_2(4,5\text{-diazafluorene})^{2+}$. This effect has dramatic consequences for the luminescence properties at room temperature where the yield of $^3\text{MLCT} \rightarrow ^3\text{LF}$ crossing (followed by fast deactivation) is estimated to be 0.79 for $\text{Ru}(\text{bpy})_3^{2+}$ and 0.99998 for $\text{Ru}(\text{bpy})_2(4,5\text{-diazafluorene})^{2+}$. In practice, no room temperature luminescence could be observed for $\text{Ru}(\text{bpy})_2(4,5\text{-diazafluorene})^{2+}$, and the lifetime of its $^3\text{MLCT}$ level was estimated to be (from extrapolation of low-temperature data) ca. 70 ps^{26} .

Although the $\text{Os}(\text{bpy})_2(4,5\text{-diazafluorene})^{2+}$ complex has never been prepared, it is easy to predict that its luminescence behavior should be substantially identical to that of $\text{Os}(\text{bpy})_3^{2+}$. Os^{II} , in fact, exhibits a considerably stronger

ligand field than Ru^{II} , so that the ${}^3\text{MLCT} \rightarrow {}^3\text{LF}$ crossing should remain inaccessible even in the $\text{Os}(\text{bpy})_2(4,5\text{-diazafluorene})^{2+}$ unit.

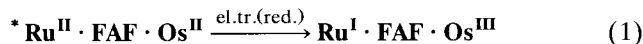
On the basis of the above arguments we can now discuss the properties of the dinuclear complexes.

The luminescence behavior of $\text{Ru}^{\text{II}} \cdot \text{FAF} \cdot \text{Ru}^{\text{II}}$, is exactly that expected from the behavior of the mononuclear $\text{Ru}(\text{bpy})_2(4,5\text{-diazafluorene})^{2+}$ model compound, *i.e.* strong and long-lived luminescence at 77K and extremely weak and short-lived luminescence at room temperature. For $\text{Os}^{\text{II}} \cdot \text{FAF} \cdot \text{Os}^{\text{II}}$, the luminescence is also relatively strong and long-lived at room temperature, confirming that the low ligand-field strength of the 4,5-diazafluorene ligand does not affect the rate of radiation-less decay at room temperature (*vide supra*).

The interaction between the metal-based units of the dinuclear complexes is certainly very weak, as shown by: (i) the identical oxidation potentials of the Ru-based moieties in $\text{Ru}^{\text{II}} \cdot \text{FAF} \cdot \text{Ru}^{\text{II}}$ and $\text{Ru}^{\text{II}} \cdot \text{FAF} \cdot \text{Os}^{\text{II}}$ and of the Os-based moieties in $\text{Os}^{\text{II}} \cdot \text{FAF} \cdot \text{Os}^{\text{II}}$ and $\text{Ru}^{\text{II}} \cdot \text{FAF} \cdot \text{Os}^{\text{II}}$; (ii) the practically identical absorption spectra exhibited by the mixed-metal $\text{Ru}^{\text{II}} \cdot \text{FAF} \cdot \text{Os}^{\text{II}}$ complex and the 1/1 mixture of its homometallic "parent" complexes $\text{Ru}^{\text{II}} \cdot \text{FAF} \cdot \text{Ru}^{\text{II}}$ and $\text{Os}^{\text{II}} \cdot \text{FAF} \cdot \text{Os}^{\text{II}}$. The absence of intense ($\epsilon > 50 \text{ M}^{-1} \cdot \text{cm}^{-1}$) intervalence transfer bands in the mixed-valence compounds confirms the lack of strong intercomponent interaction. It should be recalled, however, that even an interaction of a few cm^{-1} (which cannot be noticed in spectroscopic and electrochemical experiments) is sufficient to cause fast intercomponent energy- and electron-transfer processes⁵.

Intercomponent energy transfer in $\text{Ru}^{\text{II}} \cdot \text{FAF} \cdot \text{Os}^{\text{II}}$

In a rigid matrix at 77K, the luminescence of the Ru-based unit of $\text{Ru}^{\text{II}} \cdot \text{FAF} \cdot \text{Os}^{\text{II}}$ is almost completely quenched by the Os-based unit (Figure 4, Table II). In principle, the quenching could be due to electron- or energy-transfer processes (Figure 6a). From the excited-state energy of the Ru-based unit (2.15 eV)²⁹ and the redox potentials shown in Table I it can be estimated³⁰ that the reductive quenching process in Eqn. 1

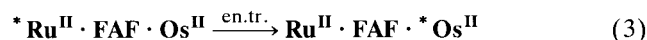


would be slightly exoergonic (-0.08 eV) and that the oxidative quenching process in Eqn. 2



would be strongly endoergonic ($+0.38 \text{ eV}$). Therefore, quenching by electron transfer, which would also imply a large reorganizational energy in polar solvents, cannot

take place. By contrast, quenching via energy transfer (Eqn. 3)



is very likely because it is exoergonic (-0.40 eV) and does not need much reorganizational energy. Evidence for energy transfer is also obtained from a comparison between the luminescence intensities of $\text{Ru}^{\text{II}} \cdot \text{FAF} \cdot \text{Os}^{\text{II}}$ and $\text{Os}^{\text{II}} \cdot \text{FAF} \cdot \text{Os}^{\text{II}}$, which shows that excitation of the Ru-based unit in the former complex leads to the luminescence of the Os-based unit.

The rate constant for energy transfer can be calculated from Eqn. 4

$$k = \frac{1}{\tau} - \frac{1}{\tau^0} \quad (4)$$

where τ and τ^0 are the luminescence lifetimes of the Ru-based component in $\text{Ru}^{\text{II}} \cdot \text{FAF} \cdot \text{Os}^{\text{II}}$ and $\text{Ru}^{\text{II}} \cdot \text{FAF} \cdot \text{Ru}^{\text{II}}$, respectively. From the lifetime values shown in Table II, k can be calculated to be $2.6 \cdot 10^8 \text{ s}^{-1}$ at 77K. The rate of the energy-transfer process is not expected to change much with temperature. Therefore, at room temperature, energy transfer can hardly compete with the intrinsic radiation-less decay rate of the Ru-based unit ($k_d = 3.3 \cdot 10^9 \text{ s}^{-1}$, as evaluated from the luminescence lifetime of $\text{Ru}^{\text{II}} \cdot \text{FAF} \cdot \text{Ru}^{\text{II}}$). The luminescence lifetime of the Ru-based unit of $\text{Ru}^{\text{II}} \cdot \text{FAF} \cdot \text{Os}^{\text{II}}$ is the same, within experimental error, as that of $\text{Ru}^{\text{II}} \cdot \text{FAF} \cdot \text{Ru}^{\text{II}}$ and the corrected excitation spectrum shows that under such conditions excitation in the Ru-based unit does not lead to significant emission from the Os-based unit.

Intercomponent electron transfer in mixed-valence compounds

Partial oxidation of $\text{Os}^{\text{II}} \cdot \text{FAF} \cdot \text{Os}^{\text{II}}$ and $\text{Ru}^{\text{II}} \cdot \text{FAF} \cdot \text{Os}^{\text{II}}$ leads to the $\text{Os}^{\text{II}} \cdot \text{FAF} \cdot \text{Os}^{\text{III}}$ and $\text{Ru}^{\text{II}} \cdot \text{FAF} \cdot \text{Os}^{\text{III}}$ mixed-valence species where the oxidized unit quenches the luminescence of the non-oxidized one. As we have seen above, in the case of $\text{Ru}^{\text{II}} \cdot \text{FAF} \cdot \text{Os}^{\text{II}}$ selective oxidation of the Os-based unit can be achieved. The luminescence from this unit ($\lambda_{\text{em}} 710 \text{ nm}$) decreases linearly on addition of the oxidant (which converts the emissive Os^{II} -based unit into the non-absorbing and non-emissive Os^{III} -based one) and, as expected, disappears after the addition of one equivalent of oxidant. In the oxidized $\text{Ru}^{\text{II}} \cdot \text{FAF} \cdot \text{Os}^{\text{III}}$ species the lifetime of the excited Ru-based unit is 240 ps. This shows that the luminescent Ru-based excited state is quenched by the Os^{III} -based component with rate constant $8.3 \cdot 10^8 \text{ s}^{-1}$ (calculated by Eqn. 4). The energy-level diagram, schematized in Figure

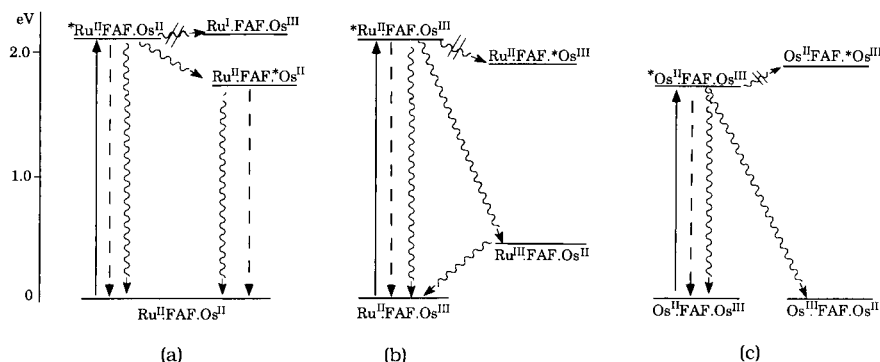


Figure 6. Energy level diagrams showing the photoinduced energy and electron-transfer processes in $\text{Ru}^{\text{II}} \cdot \text{FAF} \cdot \text{Os}^{\text{II}}$ (a), $\text{Ru}^{\text{II}} \cdot \text{FAF} \cdot \text{Os}^{\text{III}}$ (b), and $\text{Os}^{\text{II}} \cdot \text{FAF} \cdot \text{Os}^{\text{III}}$ (c). Key: full line, excitation; dashed line, luminescence; wavy line, radiation-less decay.

Table III Rate constants ^a.

	T (K)	k (s ⁻¹)	ΔG° (eV)
energy transfer:			
*Ru ^{II} ·FAF·Os ^{II} → Ru ^{II} ·FAF·*Os ^{II}	77 ^b	2.6·10 ⁸	-0.40
*Ru ^{II} ·BSB·Os ^{II} → Ru ^{II} ·BSB·*Os ^{II}	77 ^b	3.2·10 ⁷	-0.35
	298 ^c	5.0·10 ⁷	-0.35
electron transfer:			
*Os ^{II} ·FAF·Os ^{III} → Os ^{III} ·FAF·Os ^{II}	298 ^d	3.9·10 ⁸	-1.75
*Os ^{II} ·BSB·Os ^{III} → Os ^{III} ·BSB·Os ^{II}	298 ^d	5.0·10 ⁹	-1.71
*Ru ^{II} ·FAF·Os ^{III} → Ru ^{III} ·FAF·Os ^{II}	298 ^d	8.3·10 ⁸	-1.69
*Ru ^{II} ·BSB·Os ^{III} → Ru ^{III} ·BSB·Os ^{II}	298 ^d	8.7·10 ⁹	-1.62
Ru ^{III} ·FAF·Os ^{II} → Ru ^{II} ·FAF·Os ^{III}	298 ^d	2.9·10 ⁷	-0.46
Ru ^{III} ·BSB·Os ^{II} → Ru ^{II} ·BSB·Os ^{III}	298 ^d	1.0·10 ⁶	-0.44

^a M.BSB.M are the [(bpy)₂M(bpy-s-bpy)M(bpy)₂]⁴⁺ of the bpy-s-bpy bridging ligand shown in Figure 1; data taken from Ref. 14. ^b Butyronitrile glass. ^c Acetonitrile solution. ^d Acetonitrile/water solution.

6b, shows that, in principle, the quenching of the *Ru^{II}·FAF·Os^{III} luminescent excited state can take place (i) by intercomponent energy transfer to form the Ru^{II}·FAF·*Os^{III} species (where the Os^{III}-based excited state is LMCT in nature³¹) which will then relax to the ground state, or (ii) by intercomponent electron transfer via the intervalence-transfer excited state Ru^{III}·FAF·Os^{II}. Laser-flash-photolysis experiments showed that electron transfer quenching takes place, leading to Ru^{III}·FAF·Os^{II} (Figure 5) which then decays (Figure 5, inset) to its intervalence transfer ground state isomer Ru^{II}·FAF·Os^{III} with rate constant 2.9·10⁷ s⁻¹ (Figure 6b).

In the case of Os^{II}·FAF·Os^{III}, the luminescence lifetime of the Os^{II} unit is 2.4 ns, compared to the value of 41 ns found for the non-oxidized Os^{II}·FAF·Os^{II} species. By means of Eqn. 4 one can obtain a value of 3.9·10⁸ s⁻¹ for the rate constant of the quenching process. In this case (Figure 6c), energy transfer is endoergonic (~0.3 eV)³¹ and the observed intercomponent quenching process is again due to electron transfer.

The rate constants measured for the observed energy and electron-transfer processes are presented in Table III, where the corresponding data previously obtained for the analogous complexes containing the rigid -HC=CH-bco-HC=CH-¹⁴ bridging ligand (bco is bicyclo[2.2.2]octane) are also shown for purposes of comparison. A detailed discussion of these as well as other data in the light of the current theories for energy- and electron-transfer processes will be given elsewhere.

Conclusions

We have prepared a novel linear and rigid bridging ligand (diazf-a-diazf) which contains two 4,5-diazafluorene chelating units separated by an adamantane spacer. Its dinuclear complexes [(bpy)₂Ru(diazf-a-diazf)Ru(bpy)₂]⁴⁺ (Ru^{II}·FAF·Ru^{II}), [(bpy)₂Os(diazf-a-diazf)Os(bpy)₂]⁴⁺ (Os^{II}·FAF·Os^{II}), and [(bpy)₂Ru(diazf-a-diazf)Os(bpy)₂]⁴⁺ (Ru^{II}·FAF·Os^{II}) have been prepared and their absorption spectra, luminescence properties, and electrochemical behavior investigated. The absorption spectrum and redox potentials of each metal-based unit are unaffected by the presence of the other unit, consistent with a weak interchromophoric interaction. In the Ru^{II}·FAF·Os^{II} compound, photoinduced energy transfer from the Ru^{II}-based to the Os^{II}-based luminescent ³MLCT levels takes place at 77K with rate constant 2.6·10⁸ s⁻¹. At room temperature the intrinsic decay of the Ru-based unit (3.3·10⁹ s⁻¹) is too fast to allow the occurrence of energy transfer. In the mixed-valence Ru^{II}·FAF·Os^{III} and Os^{II}·FAF·Os^{III} compounds, the oxi-

dized metal-based unit quenches, by electron transfer, the luminescent excited state of the unit that is not oxidized. The rate constants for the *Ru^{II}·FAF·Os^{III} → Ru^{III}·FAF·Os^{II}, *Os^{II}·FAF·Os^{III} → Os^{III}·FAF·Os^{II} and Ru^{III}·FAF·Os^{II} → Ru^{II}·FAF·Os^{III} processes are 8.3·10⁸ s⁻¹, 3.9·10⁸ s⁻¹, and 2.9·10⁷ s⁻¹, respectively.

The novel bi-chelating ligand is very appealing as a rigid and linear bridging ligand for the construction of nanostructures based on metal complexes. However, the short excited-state lifetime at room temperature of the Ru^{II} complexes containing this ligand is somewhat disappointing. Research is in progress to design and synthesize a new bi-chelating bridging ligand exhibiting the structural advantages (rigidity and linearity) of diazf-a-diazf, whose chelating units have a ligand-field strength comparable to that of bpy.

Acknowledgements

We would like to thank Mr. *Alessandro Piretti* for his collaboration in the experiments and Mr. *M. Minghetti* for technical assistance. This work was supported by the Italian MURST and CNR (Progetto Strategico "Tecnologie Chimiche Innovative"), by the Swiss National Science Foundation, and by the European Community Program, Action COST: D4.

References and notes

- 1 V. Balzani, L. Moggi and F. Scandola, in "Supramolecular Photochemistry", V. Balzani ed., Reidel, Dordrecht, 1987, p. 1.
- 2 G.L. Closs and J.R. Miller, *Science* **240**, 440 (1988).
- 3 F. Scandola, M.T. Indelli, C. Chiorboli and C.A. Bignozzi, *Top. Curr. Chem.* **158**, 73 (1990).
- 4 D. Gust and T.A. Moore, *Topics Curr. Chem.* **159**, 103 (1991).
- 5 V. Balzani and F. Scandola, "Supramolecular Photochemistry", Horwood, Chichester, 1991.
- 6 M.R. Wasielewski, *Chem. Rev.* **92**, 435 (1992).
- 7 R.A. Bissel, A.P. de Silva, H.Q.N. Gunaratne, P.L.M. Lynch, G.E.M. Maguire and K.R.A.S. Sandanayake, *Chem. Soc. Rev.* **21**, 187 (1992).
- 8 V. Balzani and F. Scandola in "Comprehensive Supramolecular Chemistry", Volume 10, D.N. Reinhoudt, ed. Pergamon, New York, in press.
- 9 G. Denti, S. Campagna, S. Serroni, M. Ciano and V. Balzani, *J. Am. Chem. Soc.* **114**, 2944 (1992); S. Serroni, G. Denti, S. Campagna, A. Juris, M. Ciano and V. Balzani, *Angew. Chem. Int. Ed. Engl.* **31**, 1495 (1992).
- 10 For some recent papers, see:
 - a J.-P. Collin, S. Guillerez, J.-P. Sauvage, F. Barigelletti, L. De Cola, L. Flamigni, and V. Balzani, *Inorg. Chem.* **30**, 4230 (1991);
 - b S.L. Mecklenburg, B.M. Peek, J.R. Schoonover, D.G. McCafferty, C.G. Wall, B.W. Erikson, and T.J. Meyer, *J. Am. Chem. Soc.* **115**, 5479 (1993);
 - c W.E. Jones, Jr., C.A. Bignozzi, P. Chen, and T.J. Meyer, *Inorg. Chem.* **32**, 1167 (1993);
 - d M.K. Nazeeruddin, A. Kay, I. Rodicio, R. Humphry-Baker, E. Müller, P. Liska, N. Vlachopoulos, and M. Grätzel, *J. Am. Chem. Soc.* **115**, 638 (1993);
 - e E.H. Yonemoto, Y.I. Kim, R.H. Schmehl, J.O. Wallin, B.A. Shoulters, B.R. Richardson, J.F. Haw, and T.E. Mallouk, *J. Am. Chem. Soc.* **116**, 10563 (1994).
- 11a A. Juris, V. Balzani, F. Barigelletti, S. Campagna, P. Belser, and A. von Zelewsky, *Coord. Chem. Rev.* **84**, 85 (1988);
 - b E.M. Kober, J.V. Caspar, B.P. Sullivan, and T.J. Meyer, *Inorg. Chem.* **27**, 4587 (1988), and references therein;
 - c V. Balzani, F. Barigelletti, and L. De Cola, *Top. Curr. Chem.*, **158**, 31 (1990);
 - d K. Kalyanasundaram, "Photochemistry of Polypyridine and Porphyrin Complexes", Academic Press, London, 1992.
- 12a A.J. Downard, G.E. Honey, L.F. Phillips, and P.J. Steel, *Inorg. Chem.* **30**, 2259 (1991);
 - b J.-P. Gisselbrecht, M. Gross, J.-M. Lehn, J.-P. Sauvage, R. Ziessel, C. Piccinni-Leopardi, J.M. Arrieta, G. Germain, and M. van Meerssche, *Nouv. J. Chem.* **8**, 661 (1984).

- ¹³ For some recent papers, see:
- ^a S. Van Wallendaël and D.P. Rillema, *J. Chem. Soc., Chem. Commun.* 1081 (1990);
- ^b M. Furue, M. Hirata, S. Kinoshita, T. Kushida, and M. Kamachi, *Chem. Lett.* 2065 (1990);
- ^c M. Furue, K. Maruyama, Y. Kanematsu, T. Kushida, and M. Kamachi, *Coord. Chem. Rev.* **132**, 201 (1994).
- ¹⁴ L. De Cola, V. Balzani, F. Barigelletti, L. Flamigni, P. Belser, A. von Zelewsky, M. Frank and F. Vögtle, *Inorg. Chem.* **32**, 5258 (1993).
- ¹⁵ F. Vögtle, M. Frank, M. Nieger, P. Belser, A. von Zelewsky, V. Balzani, F. Barigelletti, L. De Cola, and L. Flamigni, *Angew. Chem. Int. Ed. Engl.* **32**, 1643 (1993).
- ¹⁶ F. Barigelletti, L. Flamigni, V. Balzani, J.-P. Collin, J.-P. Sauvage, A. Sour, E.C. Constable and A.M.W. Cargill Thompson, *J. Am. Chem. Soc.* **116**, 7692 (1994);
J.-P. Sauvage, J.-P. Collin, J.-C. Chambron, S. Guillerez, V. Balzani, F. Barigelletti, L. De Cola and L. Flamigni, *Chem. Rev.* **94**, 993 (1994).
- ^{17a} A. Juris, V. Balzani, P. Belser, and A. von Zelewsky, *Helv. Chim. Acta* **64**, 2175 (1981);
- ^b C.T. Lin, W.J. Boettcher, M. Chou, C. Creutz, and N. Sutin, *J. Am. Chem. Soc.* **98**, 6536 (1976).
- ¹⁸ J. Janku and S. Landa, *Coll. Czech. Chem. Commun.* **35**, 375 (1979).
- ¹⁹ L.J. Henderson, Jr., F.R. Fronczek and W.R. Cherry, *J. Am. Chem. Soc.* **106**, 5876 (1984).
- ²⁰ J.W. Greidanus, *Can. J. Chem.* **48**, 3530 (1970).
- ²¹ B.P. Sullivan, D.J. Salmon and T.J. Meyer, *Inorg. Chem.* **17**, 3334 (1978).
- ²² P.A. Lay, A.M. Sargeson, and H. Taube, *Inorg. Synth.* **24**, 291 (1986).
- ²³ D.M.P. Mingos and D.R. Baghurst, *J. Organomet. Chem.* **348**, C57 (1990).
- ²⁴ P. Belser, A. von Zelewsky, M. Frank, Ch. Seel, F. Vögtle, L. De Cola, F. Barigelletti, and V. Balzani, *J. Am. Chem. Soc.* **115**, 4076 (1993).
- ²⁵ L.J. Henderson, Jr. and W.R. Cherry, *J. Photochem.* **28**, 143 (1985).
- ²⁶ W.M. Wacholtz, R.A. Auerbach, R.H. Schmehl and M. Ollino, *Inorg. Chem.* **24**, 1758 (1985).
- ²⁷ P. Belser, A. von Zelewsky, A. Juris, F. Barigelletti and V. Balzani, *Chem. Phys. Lett.* **104**, 100 (1984).
- ²⁸ G.M. Bryant and J.E. Fergusson, *Aust. J. Chem.* **24**, 275 (1971).
- ²⁹ Excited-state energies have been estimated as the energy of the emission maximum at 77K. Other methods give more refined but substantially equivalent results.
- ³⁰ V. Balzani, F. Bolletta, M.T. Gandolfi, and M. Maestri, *Topics Curr. Chem.* **75**, 1 (1978).
- ³¹ The maximum of the lowest energy-absorption band for Os(bpy)₃³⁺ is at 2.02 eV²⁸. The zero-zero transition is expected to be 0.2–0.3 eV lower in energy.
-